# Generation of Harmonics by Sea Breeze in Nontidal Water Bodies

ADELE MILITELLO AND NICHOLAS C. KRAUS

*U.S. Army Engineer Research and Development Center, Coastal and Hydraulics Laboratory, Vicksburg, Mississippi*

4 January 2000 and 12 January 2001

ABSTRACT

The sea breeze introduces harmonics of its diurnal cycle into water bodies, which can be notable for strong sea breeze and microtidal and nontidal conditions. The harmonics can be of the same magnitude as those produced by bottom friction and dominate those produced by nonlinear terms in the equations of motion. A closed-form analytic solution of the linearized depth-averaged equations of motion including friction is discussed for the situation of a sea breeze blowing on an idealized one-dimensional basin of constant depth. The solution reveals the generation of odd harmonics introduced by the quadratic wind stress and role of (linearized) friction. Sea-breeze forcing on the idealized basin is numerically modeled, and agreement with the analytic solution is found. The numerical model is then run with quadratic bottom friction and nonlinear terms to compare relative contributions to the generation of harmonics. Harmonics of the water motion are distinguished as *forced,* or arising from the wind forcing, and as *response,* or arising from the interactions within the water. The hydrodynamics of Baffin Bay, Texas, are modeled and spatial variation and relative strength of the harmonics investigated. Baffin Bay is a large shallow embayment with a weak connection to the Gulf of Mexico that experiences a strong southeast wind and sea breeze during the summer. The wind induces even and odd forced harmonics through the combined quasi-steady southeast wind and sea breeze. At Baffin Bay, ratios of the semidiurnal to diurnal amplitudes of water level and current speed are found to be comparable to $M_4/M_2$ ratios for U.S. Atlantic coast embayments.

## 1. Introduction

Sea breezes induce diurnal water motion in coastal embayments. Because wind forces the water as a quadratic function of its speed, harmonics of motion generated by a sea breeze are present in the water level and current, in addition to the fundamental forcing frequency. These harmonics are termed *forced* herein, because they enter directly through of the surface stress and are not an outcome of interactions within the water.

Nonlinear interactions within the water body also transfer energy into harmonic frequencies, as shown in numerous studies of tidal motion (e.g., Dronkers 1964; Boone and Byrne 1981; Uncles 1981; Speer and Aubrey 1985; Parker 1991; Friedrichs and Madsen 1992; Godin 1999). In two-dimensional, depth-averaged horizontal flow, the quadratic bottom stress, advection, and nonlinear continuity terms generate harmonics. Even harmonics are generated by the advection and nonlinear continuity terms, and by the portion of the friction term containing the water-surface elevation, whereas the quadratic velocity portion of the friction term generates odd harmonics (Parker 1991). A pure sinusoidal wind generates odd harmonics. Even and odd harmonics of the fundamental forcing frequencies of the wind and the tide are generated by nonlinear interactions within the water, and these are termed *response* harmonics herein.

Wind forces water motion locally. This situation contrasts with tidal forcing, which occurs at the ocean boundaries. Therefore, harmonics introduced by the wind can remain at full strength where they force the motion in the water body, as opposed to tidal harmonics that are generated during propagation and decay with distance to a particular location in a water body.

The sea breeze fluctuates with a frequency of 1 cpd, close to frequencies of diurnal tidal constituents ($K_1$, $O_1$, $S_1$, and others). Similarly, higher harmonics of the water motion induced by the sea breeze (referred to herein as *wind harmonics*) lie at frequencies near higher harmonics of the diurnal tidal frequencies. Thus, wind harmonics can be obscured by tidal motion and may not be easily detected. Conversely, tidal constituents must be calculated carefully if wind harmonics are present because they introduce similar motion not of gravitational origin (Zetler 1971). In microtidal embayments,

*Corresponding author address:* Dr. Adele Militello, U.S. Army Engineer Research and Development Center, Coastal and Hydraulics Laboratory (CEERD-HN-C), 3909 Halls Ferry Road, Vicksburg, MS 39180-6199.
E-mail: adele.militello@erdc.usace.army.mil

the sea breeze can contribute significantly to the diurnal variance of the water surface and current. This situation is common along the coast of Texas, where the strong predominant southeast wind and sea breeze can dominate the tide in producing setup and setdown in its numerous shallow estuaries and bays (Collier and Hedgpeth 1950).

The present study examines oscillatory wind forcing on narrow (nonrotational) water bodies. First, the presence of wind harmonics is demonstrated in a closed-form solution of the depth-averaged linearized equations of motion describing an idealized basin. The analytic model serves to validate the numerical model applied in this study. Then wind-forced hydrodynamics of Baffin Bay, Texas, are investigated through measurement and numerical modeling. During the summer, a well-developed sea breeze at Baffin Bay is superposed on a persistent southeast wind. Because the bay does not experience diurnal and semidiurnal tidal motion (Gill et al. 1995), it is a convenient location to study wind harmonics without the complication of a dominant tide.

## 2. Wind harmonics

A spatially uniform oscillatory wind blowing parallel to the $x$ axis is specified. The wind speed $W$ is then given as

$$W = w_0 + w \sin(\sigma t), \tag{1}$$

where $w_0$ is the speed of the steady wind, $w$ is the amplitude of the oscillatory wind, $\sigma = 2\pi/T$ in which $T$ is the period of the oscillatory wind, and $t$ is time. A sinusoidal representation for the wind with $T = 24$ h is a reasonable representation of the sea breeze (Hsu 1970).

To demonstrate how harmonics are generated through wind forcing, for the special case $W \geq 0$, the quadratic wind velocity is

$$|W|W = W^2 = w_0^2 + \frac{1}{2}w^2 + 2w_0 w \sin(\sigma t) - \frac{1}{2}w^2 \cos(2\sigma t). \tag{2}$$

Equation (2) contains three components as forcing by a steady part, by the fundamental diurnal frequency $\sigma$, and by the first even harmonic (semidiurnal frequency) $2\sigma$ of the fundamental. Superposition of a steady wind and an oscillatory wind is revisited in discussion of Baffin Bay.

For a pure oscillatory wind, $w_0 = 0$, and the Fourier expansion (Prandle 1991) of the quadratic wind velocity produced by (2) is

$$|W|W = w^2 \sum_{j=1}^{\infty} A_j \sin[(2j - 1)\sigma t] \tag{3}$$

in which

$$A_j = \frac{-8}{\pi(2j - 3)(2j - 1)(2j + 1)}. \tag{4}$$

Thus, harmonic frequencies generated by a pure oscillatory wind are odd multiples of the fundamental frequency. The relative magnitudes of $A_2$ and $A_3$ to $A_1$ are 1/5 and 1/35.

## 3. Scaling analysis

A scaling analysis of the one-dimensional depth-averaged equations of motion is performed to understand the relative strengths of the individual terms in the momentum equation with respect to the wind-forcing term. Local forcing by wind creates relative strengths different than classical forcing by tides at a boundary. Bottom friction dominates in shallow tidal embayments without wind, as shown by the scaling analysis of Friedrichs and Madsen (1992) and Friedrichs and Aubrey (1994). The present work contrasts with that work by demonstrating that the friction and wind terms are comparable and together are the dominant terms.

For a basin of uniform width such that water depth $h$ is much greater than the deviation from the still-water level $\eta$, the continuity and momentum equations are

$$\frac{\partial \eta}{\partial t} + \frac{\partial (hu)}{\partial x} = 0 \tag{5}$$

$$\frac{\partial u}{\partial t} + u\frac{\partial u}{\partial x} + g\frac{\partial \eta}{\partial x} + \frac{C_b|u|u}{h} + \frac{\rho_a}{\rho}\frac{C_w|W|W}{h} = 0, \tag{6}$$

where $\eta$ is the deviation from the still-water level, $h$ is the still-water depth, $x$ is the horizontal coordinate, $u$ is the depth-averaged current velocity, $g$ is the gravitational acceleration, $C_b$ is an empirical bottom-stress coefficient, $C_w$ is a wind-drag coefficient, $\rho_a$ is the density of air, $\rho$ is the density of water, and $W$ is the component of the wind velocity parallel to the $x$ axis.

Equations (5) and (6) are expressed in characteristic scales (Friedrichs and Madsen 1992) as

$$\frac{a}{T} + \frac{hU}{L} = 0 \tag{7}$$

$$\frac{U}{T} + \frac{U^2}{L} + \frac{ga}{L} + \frac{C_b U^2}{h} + \frac{\rho_a}{\rho}\frac{C_w W^2}{h} = 0. \tag{8}$$

Here $a$ is the amplitude of the water surface elevation forced by the sea breeze, $U$ is the amplitude of the sea-breeze-forced velocity, $W$ is the amplitude of the sea breeze wind speed, $T$ is the period of the sea breeze, and $L$ is the length of the basin. From (7) and (8), the scales of friction $F_F$, wind $F_W$, pressure gradient $F_P$, and inertial $F_I$ terms are

$$F_F = \frac{C_b U^2}{h}, \qquad F_W = \frac{\rho_a}{\rho}\frac{C_w W^2}{h}, \qquad F_P = \frac{ga^2}{hUT},$$

$$F_I = \frac{U}{T}. \tag{9}$$

The ratio of friction to wind scales is

$$\frac{F_F}{F_W} = \frac{C_b U^2}{\frac{\rho_a}{\rho} C_w W^2} \tag{10}$$

for which there is no depth dependence. To obtain the wind-stress coefficient for shallow water, we apply the formulation of Hsu (1988),

$$C_w = \left(\frac{\kappa}{14.56 - 2 \ln W_{10}}\right)^2, \tag{11}$$

where $\kappa$ is von Kármán's constant and $W_{10}$ is the wind speed 10 m above the water surface. For a representative sea breeze amplitude of $W = W_{10} = 3$ m s$^{-1}$, $C_w = 0.0010$. For sea-breeze-forced shallow water, $T = 8.64 \times 10^4$, $U \approx 0.05$ m s$^{-1}$, $a \approx 0.05$ m, and $C_b \approx 0.005$. Scaling with these representative values gives $F_F/F_W = 1$, $F_I/F_W = 0.05$, and $F_P/F_W = 0.5$. The analysis shows that friction and wind terms are the same order of magnitude. The pressure gradient is the same order of magnitude as the wind and friction terms, whereas the inertial term is two orders of magnitude smaller. Similar analysis for the advective terms shows that they are three orders of magnitude smaller than the wind term for the stated conditions.

## 4. Wind forcing on an idealized basin

An idealized basin was considered to obtain a closed-form solution for investigating the generation of forced wind harmonics. An analytic solution reveals functional dependencies governing the generation of wind harmonics and provides insight for interpreting numerical solutions required to model water bodies under realistic conditions.

The one-dimensional basin with vertical walls has length $L$ and uniform still-water depth, over which an along-axis sinusoidal wind blows with spatial uniformity. The governing equations are linearized to allow a closed-form solution and to eliminate generation of response harmonics by nonlinear terms. The linear bottom-friction coefficient $C_{bL}$ can be estimated by the principle of equivalent work (Ippen and Harleman 1966), giving $C_{bL} = (8/(3\pi))\, u_m C_b$, where $u_m$ is a representative value of the magnitude of the current. We take $u_m = (\eta_r/h)c$, with $\eta_r$ the water surface elevation range (0.1 m for Baffin Bay), $c = \sqrt{gh}$, and $h = 1$ m, giving $u_m = 0.3$ m s$^{-1}$. The quantity $C_{bL}$ has dimensions of velocity.

The continuity and momentum equations become

$$\frac{\partial \eta}{\partial t} = -h\frac{\partial u}{\partial x} \quad \text{and} \tag{12}$$

$$\frac{\partial u}{\partial t} = -g\frac{\partial \eta}{\partial x} - \frac{C_{bL}}{h}u + C_w\frac{\rho_a}{\rho}\frac{|W|W}{h} \tag{13}$$

for pure oscillatory wind specified by (1) with $w_0 = 0$. Although the wind drag coefficient varies with the wind speed in some formulations (e.g., Charnock 1955; Wu 1980; Hsu 1988; Garrett 1992), it is taken to be constant for the analytical solution.

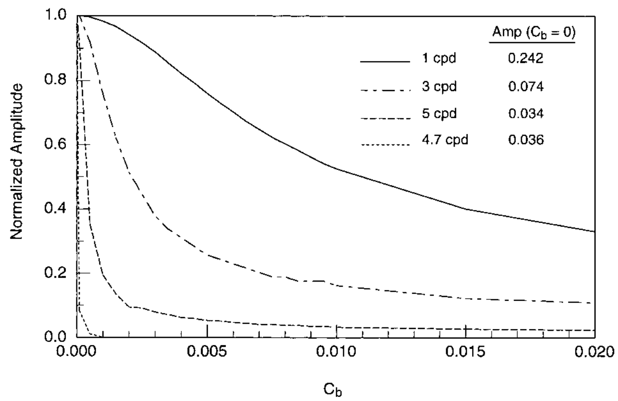


FIG. 1. Analytical solution with linear friction: normalized amplitude for oscillatory wind-forced water level for friction coefficient ranging from 0 to 0.020.

### a. Analytic solution

We solve (12) and (13) by cross-differentiation (Lamb 1945; Ippen and Harleman 1966) to give the one-dimensional inhomogeneous wave equation, which can be solved by the Fourier method (Kraus and Militello 2001). Initial and boundary conditions are $u(x, 0) = u_t(x, 0) = 0$ and $u(0, t) = u(L, t) = 0$. The water surface is specified to be initially horizontal, and the wind begins blowing at $t = 0$. The resultant analytic solution describes a linearized wind-forced motion in a one-dimensional basin as governed by water depth, basin length, bottom-friction coefficient, wind speed, and fundamental frequency of the oscillatory wind.

The geometry of the idealized basin was established as $L = 29$ km, $h = 1$ m, upon which a spatially uniform sinusoidal wind was imposed with $w = 10$ m s$^{-1}$, $C_w = 0.0016$. The number of required harmonics and normal modes was investigated. For the idealized basin, a 0.4% convergence error was obtained with five wind harmonics and seven normal modes.

With bottom friction acting, higher-mode frequencies will dissipate more steeply than for lower modes. Damping of water-surface elevation amplitudes for the friction coefficient $C_b$ ranging from 0 (no friction) to 0.02 (strong damping, as over a porous reef) are shown in Fig. 1 for the idealized basin. Amplitude values were normalized by the no-friction amplitude of the corresponding frequency. Motions on the fundamental forcing frequency (1 cpd), the second and fourth harmonics (3 and 5 cpd, respectively), and the first resonant mode (4.7 cpd) are present. Amplitudes for the fundamental and harmonic frequencies are steeply damped for smaller friction coefficients. As the friction coefficient increases, changes in amplitudes of the harmonic frequencies are reduced, indicating a balance between wind

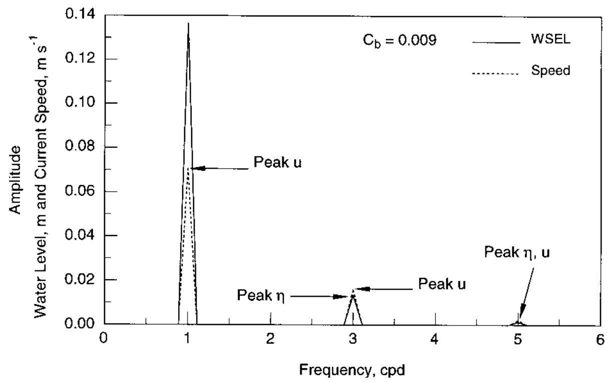


FIG. 2. Analytic solution: spectra of water-surface elevation and current, 1-m depth.

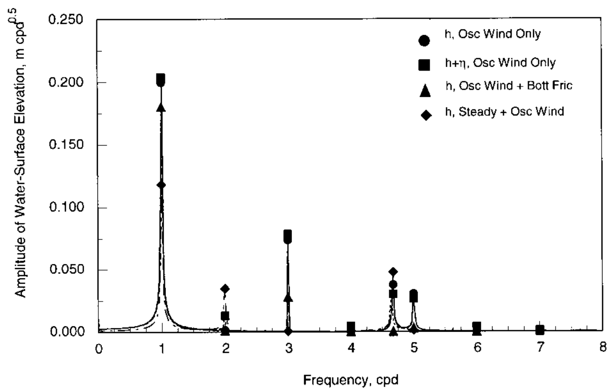


FIG. 3. Numerical solution: comparison of spectra of water-surface elevation for linear and nonlinear interactions.

and friction. Motion at these frequencies is present, even at large friction values, because it is forced over the entire surface. Motion near the resonant frequency is greatly damped for even small values of friction.

Wind-generated harmonics introduce complex structure to the water surface elevation and current velocity. The spectra of $\eta$ at the middle of the basin and of $u$ at $x = L - 500$ m for $C_b = 0.009$ are shown in Fig. 2 and indicate peak motion at the fundamental frequency of 1 cpd and energy at the harmonics 3 and 5 cpd. Amplitude ratios of the 3 cpd harmonic to the fundamental frequency are 0.10 and 0.23 for water surface elevation and current speed, respectively.

### b. Numerical solution

The idealized basin was simulated with a two-dimensional, depth-averaged, long-wave model called M2D (Militello 1998, 2000) that solves the continuity and momentum equations on a finite-difference grid. The basin was represented by a grid 29 cells long and 1 cell wide, with cell dimensions of 1000 m on each side. The oscillatory wind and the wind drag coefficient $C_w$ were the same as specified in the analytic model. For direct comparison with the analytic solution, all nonlinear terms were omitted and the friction term linearized so that the equations of motion in the numerical model reduced to (12) and (13). Error analysis comparing the analytic and numerical solutions gives rmse values for water surface elevation of 0.005 m for $C_b =$ 0.0 and 0.002 m for $C_b = 0.009$. For current speed with the same friction coefficients, the rmse values are 0.008 m s$^{-1}$ and 0.001 m s$^{-1}$. The small rmse values demonstrate that the numerical calculation is in good agreement with the analytic solution.

Simulations were conducted to examine the role of bottom friction (with linearization of the $h + \eta$ term to $h$) and nonlinear interactions on the wind-forced water level and current. Five cases were chosen (Table 1) to isolate contributions to response harmonics from the various terms. Figure 3 shows spectra for four cases. Results of cases 3 and 5 were nearly identical, so only case 3 is included. Peaks of the spectra occur at five frequencies: the fundamental wind-forcing frequency of 1 cpd (diurnal), odd harmonics of 3 and 5 cpd, even harmonic of 2 cpd (semidiurnal), and the basin mode of 4.7 cpd. At 1 cpd, $\eta$ in the wind stress (case 2) increased the amplitude slightly. Bottom friction (case 3) and the forcing of the combined steady plus oscillatory wind (case 4) reduced the amplitude of the fundamental by 9% and 40%, respectively. Reduction from the combined winds partly owes to the steady and oscillatory components being directionally opposed half of the time, reducing the resultant wind speed.

Harmonics at 3 and 5 cpd have greatest energy for the oscillatory wind-only cases (with and without $\eta$), and the peaks for these are similar, indicating that the $\eta$ nonlinearity does not contribute significantly to harmonics at these frequencies. At 5 cpd, there is almost

TABLE 1. Terms included in momentum equation for examination of harmonics produced. Linear wind and friction denotes that $\eta$ is not included in the denominator of these terms; nonlinear wind does include $\eta$ in the denominator of the wind-stress term. For oscillatory wind, $w = 3$ m s$^{-1}$, and for steady wind, $w_0 = 10$ m s$^{-1}$.

| Case | Wind | Terms and form: Bottom friction | Terms and form: Advection and finite amplitude |
|---|---|---|---|
| 1 | Oscillatory, linear | — | — |
| 2 | Oscillatory, nonlinear | — | — |
| 3 | Oscillatory, linear | Linear | — |
| 4 | Steady and oscillatory | — | — |
| 5 | Oscillatory | Linear | Included |

no energy for the situation with friction because of damping.

A harmonic at 2 cpd is present for case 2, oscillatory wind including the $\eta$ nonlinearity, and for case 4, combined steady and oscillatory wind. Inclusion of $\eta$ in the wind-stress term contributes to energy transfer to even harmonics and also agrees with the qualitative discussion of (2) for the combined steady and oscillatory winds. The amplitude of the normal mode is greatest for the combined winds, and slightly lower for the wind-only situations. With friction, the normal mode frequency is damped, as expected.

Inspection of the time series (not shown) for cases 1 and 2 indicates that inclusion of $\eta$ in the denominator of the wind stress (case 2) lowers the peaks and troughs in water surface elevation relative to the situation without $\eta$ (case 1) (enhances setdown and reduces setup). This is expected because the leading correction to the term $(h + \eta)^{-1} \cong 1 - \eta/h$ is negative. Inclusion of bottom friction (case 3) decreases amplitude of peaks and troughs notably and reduces higher-frequency oscillations overall. Bottom friction caused an 82-min lag in water surface elevation.

## 5. Dynamics of Baffin Bay, Texas

Tides along the Texas Gulf coast are diurnal, and its lagoons and shallow embayments have tidal ranges between near zero and 0.3 m (Marmer 1954; Zetler and Hansen 1970; Smith 1979). In contrast, Texas coastal embayments exhibit comparable or larger fluctuations in water level by wind (Collier and Hedgpeth 1950; Copeland et al. 1968). The Texas coast experiences strong winds as an annual southeast wind, a diurnal sea breeze during May–September, and quasiperiodic northern fronts during October–April. Copeland et al. (1968) measured water surface change by a wind of approximately 0.6 m just south of Baffin Bay in the Laguna Madre, and Kraus and Militello (1999) recorded similar magnitude fluctuations in East Matagorda Bay under forcing by wind fronts with a period of approximately 5 days. The shallow waters and narrow channels typically separating embayments from tidal inlets act as low-pass filters (Smith 1988), which can make, for example, the fortnightly component a significant contributor to the tide (Collier and Hedgpeth 1950; Smith 1985).

### *a. Study site*

Baffin Bay is a shallow, three-armed embayment located on the southern Texas coast. The principal axis of the bay is aligned approximately east–west, parallel to the predominant southeast wind. The bay is approximately 29 km long from its intersection with the Upper Laguna Madre to the western end of Cayo del Grullo. Typical depths are 2.3 m in the main body and 1.4 m in the arms. Aransas Pass, the nearest inlet, is located 60 km to the north, and water must propagate through both Corpus Christi Bay and the Upper Laguna Madre to reach Baffin Bay. The Upper Laguna Madre is a shallow (typical depth of 1 m) elongated lagoon oriented parallel to the coast. Baffin Bay is also connected to the Lower Laguna Madre (typical depth of 1 m), and its two inlets are located 70 and 125 km from the bay. Water exchange between Baffin Bay and Lower Laguna Madre takes place through wind-tidal flats dividing the upper and lower sections of the Laguna Madre via a relatively narrow navigation channel, the Gulf Intracoastal Waterway. Diurnal and semidiurnal tidal signals are severely attenuated by the great distance and shallow water between Baffin Bay and nearest inlets to the Gulf of Mexico. The mouth of Baffin Bay is classified as nontidal by National Ocean Service (NOS) standards (Gill et al. 1995), meaning that the tidal amplitude was determined to be less than approximately 0.05 m.

During the summer, the typical wind has two components, a persistent southeast wind and the sea breeze. The wind induces an along-axis water-level tilt with setup on the western end of Baffin Bay and setdown on the eastern end and in the southern Upper Laguna Madre. Sea-breeze-induced setup ranges from approximately 0.1 to 0.3 m (Militello 2000).

### *b. Measurements*

Water-level data were obtained at the three stations, Riviera, Bird Island, and Yarborough, shown in Fig. 4. Water level was recorded as a 3-min average at 6-min intervals by acoustic gauges under NOS standards. Wind velocity was measured at Yarborough, located 9 km south of the mouth of Baffin Bay and recorded hourly as a 2-min average of 1-s samples.

During August 1994, the wind was representative of typical summer conditions. Wind data for August 1994 (Fig. 5) were decomposed into north–south and east–west components and high-pass filtered with a cutoff of 30 days to remove long-period energy. The sea breeze is evident in the daily cycling, particularly in the east–west wind component. Longer-period variation of the southeast wind, on the order of days, is also present. Approximately coincident directions of the sea breeze and southeast wind enhance the peak wind speed. The spectra (Fig. 6) have two peaks, a smaller one at low frequency (less than 0.1 cpd) and a larger one at 1 cpd that represents the sea breeze. During this month, the sea breeze was primarily directed east–west. Harmonics of the sea breeze are not present in the wind spectra, indicating that (1) is a reasonable representation of the sea breeze for Baffin Bay.

Water-level data from the Riviera gauge for August 1994 were also high-pass filtered with cutoff frequency of 30 days (Fig. 7). The daily oscillations (response to sea-breeze forcing) and the fortnightly cycle of the astronomical tide are the two predominant signals. Diurnal setup at Riviera ranged from approximately 0.10 m to 0.25 m during this time interval. The spectrum of the

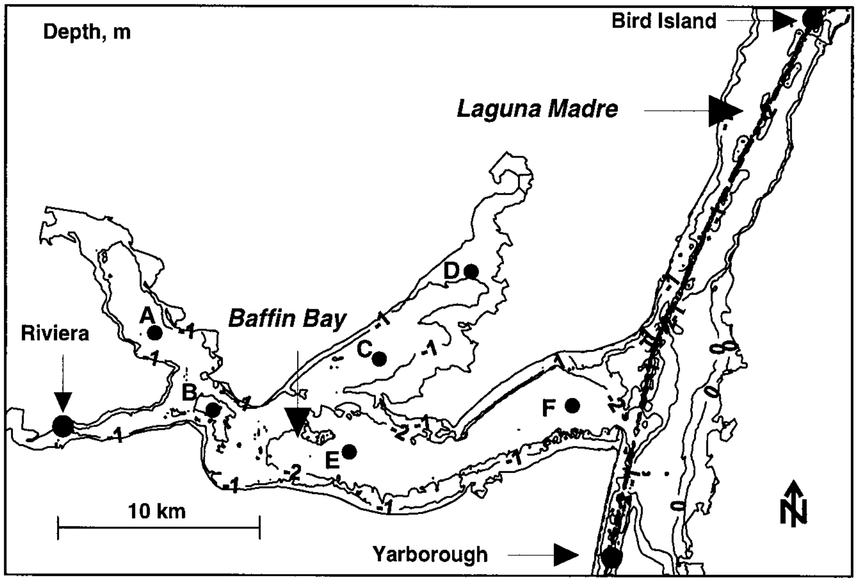


FIG. 4. Site map of Baffin Bay, Texas, showing gauge locations, numerical stations, and approximate depths.

water level for August 1994 (Fig. 8) has three peaks. The peak at 0.0645 cpd (15.5 days) corresponds to the fortnightly tide. The dominant peak at 1 cpd is a response to the sea breeze and has amplitude 0.06 m, which corresponds to a mean diurnal setup of 0.12 m. A small peak at the semidiurnal frequency 2 cpd represents the first harmonic of the diurnal motion. The amplitude of the semidiurnal peak is 0.016 m, corresponding to a mean semidiurnal setup of 0.03 m. These amplitudes give a semidiurnal to diurnal ratio of 0.27. The fundamental seiche period for Baffin Bay is approximately 3 h (8 cpd) and is not near the period of diurnal motion and its first two harmonics.

### *c. Wind harmonics in Baffin Bay*

Numerical simulation of the water level and current in Baffin Bay was conducted for the time interval 1–31 July 1995 to investigate wind harmonics and the spatial variations in semidiurnal to diurnal ratios. During this time the east–west component of the southeast wind was relatively steady so that the peak east–west wind speed did not vary significantly over the month (Fig. 9). The general pattern of east–west wind component was a west-directed wind that strengthened and weakened on a diurnal cycle. For this simulation, linear and nonlinear terms in the equations of motion were included in the computations, and the wind-stress coefficient given by (11) was applied. The full equations allow comparison of the contributions arising from all nonlinear terms and from the wind stress to harmonics in the water motion.

Spectra of the east–west and north–south components of the quadratic wind speed are shown in Fig. 10 for July 1995. The dominant energy for the east–west component appears at the diurnal frequency. The north–south component contains peak energy at the lower fre-

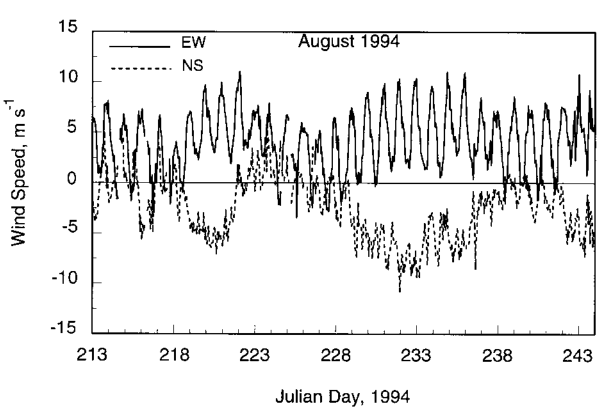


FIG. 5. Decomposed wind speed at Yarborough, Texas, for Aug 1994. North–south and east–west wind speeds are denoted by NS and EW, respectively. Positive values of the components indicate wind from the north and east.

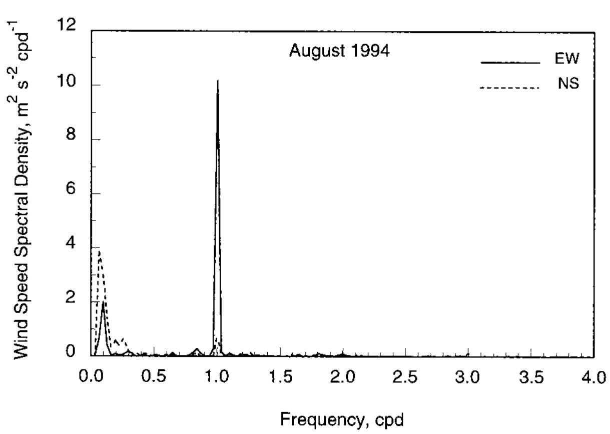


FIG. 6. Spectra of north–south and east–west wind components at Yarborough, Texas, for Aug 1994.

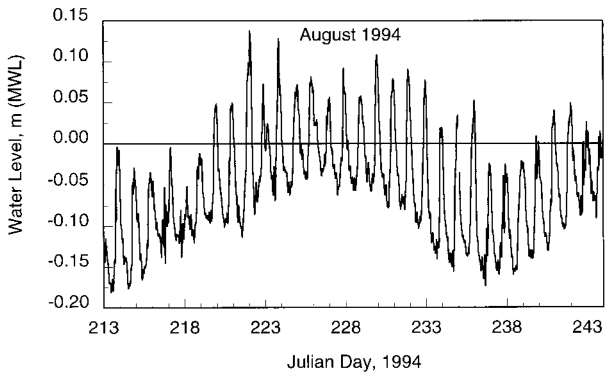


FIG. 7. Water level at Riviera, Texas, for Aug 1994.

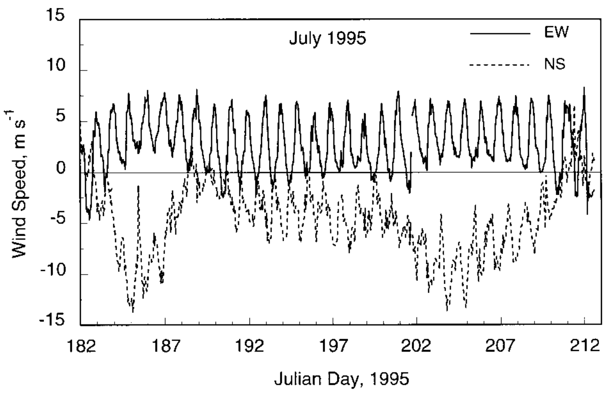


FIG. 9. Decomposed wind speed at Yarborough, Texas, for Jul 1995.

quencies of the quasi-steady southeast wind, and the energy at the diurnal frequency is similar in magnitude to that of the east–west component. For both components, energy is present at the first harmonic of the diurnal frequency ($2\sigma$) and is created by the southeast wind and sea breeze. Ratios of the semidiurnal to diurnal amplitudes of the quadratic wind components in Fig. 10 are 0.32 and 0.27 for the east–west component and the north–south component, respectively.

We introduce notation for amplitudes of motion of the wind-generated fundamental frequency and its first harmonic. The amplitude of water motion forced by the diurnal sea breeze is denoted as $W_1$ and its semidiurnal harmonic as $W_2$. This notation is convenient for describing amplitude ratios analogous to $M_4/M_2$ overtide ratios.

Six numerical stations in Baffin Bay are examined to investigate ratios of $W_2/W_1$ and the relative contribution to harmonics by the calculated nonlinear terms and wind stress. Their locations (Fig. 4) were chosen to be representative of the entire bay. Table 2 lists amplitude ratios for water level and both components of the horizontal current. The $W_2/W_1$ ratio for water level ranges from approximately 0.2 to 0.6 with lower values in the shallower sections of the bay (arms). Ratios of water-level amplitude calculated for the bay arms range from 0.19 to 0.34. These values are similar to the $W_2/W_1$ ratio of 0.27 from measurements at Riviera. Ratios for the current speed range from approximately 0.4 to 0.6, with no apparent spatial distribution. In comparison, $M_4/M_2$ overtide amplitude ratios observed in estuaries on the Atlantic coast of the United States range from near zero to approximately 0.5, with typical values of 0.1 to 0.3 (Speer et al. 1991; Friedrichs and Madsen 1992). Therefore, ratios of the 2-cpd harmonic to its fundamental frequency for wind are comparable to those for tide. In Baffin Bay, the $W_2/W_1$ ratios tend to be on the higher end of overtide ratios found for tides.

Comparison of the amplitudes of nonlinear momentum equation terms at the semidiurnal frequency revealed that the wind and bottom stresses were the same order of magnitude. The wind stress dominated the advective terms by two to three orders of magnitude at all numerical stations. A separate simulation was conducted with the nonlinear continuity terms removed from the computations and the results were compared to those with the full equations. The nonlinear continuity terms were found to contribute less than 10% of the energy at the first harmonic. Thus, the primary contributors to motion at the 2 cpd harmonic are the wind and bottom stresses. Wind produces water motion on the 2 cpd har-

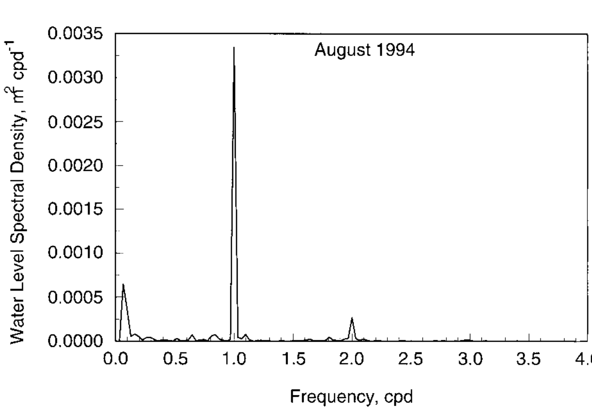


FIG. 8. Spectrum of water level at Riviera, Texas, for Aug 1994.

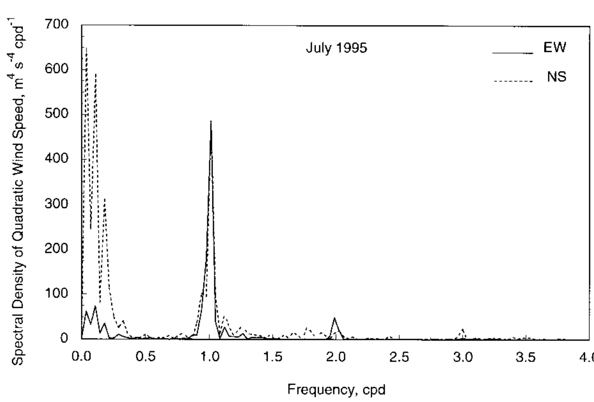


FIG. 10. Spectra of east–west and north–south components of quadratic wind speed measured at Yarborough, Texas, Jul 1995.

TABLE 2. Ratios $W_2/W_1$ for water level and horizontal current speed at numerical station locations.

| | Numerical station | | | | | |
|---|---|---|---|---|---|---|
| Variable | A | B | C | D | E | F |
| $\eta$ (m) | 0.31 | 0.34 | 0.19 | 0.26 | 0.46 | 0.57 |
| $u$ (m s$^{-1}$) | 0.55 | 0.60 | 0.38 | 0.41 | 0.57 | 0.43 |
| $v$ (m s$^{-1}$) | 0.51 | 0.58 | 0.40 | 0.41 | 0.47 | 0.52 |

monic directly by local forcing. The bottom stress is the most significant contributor to the response portion of the 2 cpd harmonic.

Because the quadratic wind stress introduces both forced and response harmonics, it was examined to determine the relative magnitude of the two contributions. Two forms of the wind stress were evaluated, one omitting $\eta$ in the denominator and the other containing $\eta$ for producing both forced and response contributions. Spectral analysis revealed that the amplitudes of the fundamental frequency and its first harmonic were nearly identical for both forms of the wind stress at all numerical stations. Thus, inclusion of $\eta$ in the wind stress does not significantly contribute to transfer of energy into higher harmonic frequencies in Baffin Bay. Harmonics at 3 cpd were not considered for analysis because their values were considered too small to be reliable.

## 6. Conclusions

This study found that a sea breeze can introduce significant harmonic motion into water bodies. The sea breeze alone generates diurnal oscillations and odd harmonics of its fundamental frequency. The sea breeze combined with a quasi-steady wind introduces semidiurnal and higher even harmonics of the diurnal wind. Two sources of wind harmonics were defined. Forced harmonics are introduced directly through the quadratic wind stress (as newly demonstrated here), and response harmonics are generated from nonlinear interactions (known from previous work). The quadratic wind stress in the momentum equations generates both forced and response harmonics, with the weaker response harmonics demonstrated to be associated with the instantaneous water surface elevation in the denominator.

Because wind harmonics are locally forced, they can be present in water motion, even with friction acting. Calculation showed that the amplitudes of wind harmonics decrease relatively steeply for smaller friction values, but become nearly constant with increased values of friction. Lack of decrease in amplitude indicates that friction and wind forcing balance for larger values of friction. This situation differs from resonant modes that can be nearly completely damped for relatively small friction.

An idealized one-dimensional basin example was introduced to study the water response to an oscillatory wind as governed by the linearized equations of motion with quadratic wind stress. Availability of the analytic solution allowed checking of the numerical model employed to simulate the depth-averaged hydrodynamics of Baffin Bay, Texas. The idealized basin served as a means of exploring the relative contributions of various terms and interactions in the equations of motion. For the examples examined, the primary contributors responsible for the generation or damping of oscillatory motion under sea-breeze forcing were the oscillatory wind and bottom friction. The nonlinear continuity terms contributed to less than 10% of the harmonic amplitudes. Contributions to generation of harmonics by the instantaneous water elevation in the nonlinear quadratic wind-forcing term and the advective terms were small. Thus, the first harmonic is composed primarily of the forced wind component and the response component generated by the bottom stress.

Numerical computation of wind-forced motion in Baffin Bay, Texas, revealed that $W_2/W_1$ ratios are comparable to $M_4/M_2$ ratios for U.S. Atlantic coast embayments. Wind forcing at Baffin Bay consists of diurnal sea breeze and a quasi-steady southeast wind. During a sea-breeze cycle in August 1994, the maximum range of water level was measured to be 0.25 m on the western end of the 2.3-m-deep, 29-km-long Baffin Bay. The analysis presented for sea breeze also extends to quasiperiodic wind-forced motion such as that associated with weather fronts.

*Acknowledgments.* The authors would like to thank Carl Friedrichs and an anonymous reviewer for comments that improved this paper. This work was conducted as part of activities of the Inlet Modeling System Work Unit of the Coastal Inlets Research Program of the U.S. Army Corps of Engineers (USACE). Permission was granted by Headquarters, USACE, to publish this information.

REFERENCES

Boon, J. D., and R. J. Byrne, 1981: On basin hypsometry and the morphodynamic response of coastal inlet systems. *Mar. Geol.,* **40,** 27–48.

Charnock, H., 1955: Wind stress on a water surface. *Quart. J. Roy. Meteor. Soc.,* **81,** 639–640.

Collier, A., and J. W. Hedgpeth, 1950: An introduction to the hydrography of tidal waters of Texas. *Pubs. Inst. Mar. Sci. Univ. Tex.,* **1** (2), 125–194.

Copeland, B., J. Thompson, and W. Ogletree, 1968: Effects of wind on water level in the Texas Laguna Madre. *Tex. J. Sci.,* **20** (2), 196–199.

Dronkers, J. J., 1964: *Tidal Computations in Rivers and Coastal Waters.* North–Holland, 518 pp.

Friedrichs, C. T., and O. S. Madsen, 1992: Nonlinear diffusion of the tidal signal in frictionally dominated embayments. *J. Geophys. Res.,* **97** (C4), 5637–5650.

——, and D. G. Aubrey, 1994: Tidal propagation in strongly convergent channels. *J. Geophys. Res.,* **99** (C2), 3321–3336.

Garrett, J. R., 1992: *The Atmospheric Boundary Layer.* Cambridge University Press, 316 pp.

Gill, S. K., J. R. Hubbard, and G. Dingle, 1995: Tidal characteristics and datums of Laguna Madre, Texas. NOAA Tech. Memo. NCS OES 008, National Oceanic and Atmospheric Administration, Silver Spring, MD, 109 pp.
Godin, G., 1999: The propagation of tides up rivers with special considerations on the Upper Saint Lawrence River. *Estuarine Coastal Shelf Sci.,* **48,** 307–324.
Hsu, S. A., 1970: Coastal air-circulation system: Observations and empirical model. *Mon. Wea. Rev.,* **98,** 487–509.
——, 1988: *Coastal Meteorology.* Academic Press, 260 pp.
Ippen, A. T., and D. R. F. Harleman, 1966: Tidal dynamics in estuaries. *Estuary and Coastline Hydrodynamics,* A. T. Ippen, Ed., McGraw-Hill, 493–545.
Kraus, N. C., and A. Militello, 1999: Hydraulic study of multiple inlet system: East Matagorda Bay, Texas. *J. Hydraul. Eng.,* **25** (3), 224–232.
——, and ——, 2001: Oscillations in a one-dimensional bay forced by sea breeze: Analytical solution and numerical model tests. *Proc. of Waves 2001,* San Francisco, CA, American Society of Civil Engineers, in press.
Lamb, H., 1945: *Hydrodynamics.* 6th ed. Dover, 738 pp.
Marmer, H. A., 1954: Tides and sea level in the Gulf of Mexico. *Fishery Bull. Fish Wildl. Serv. U.S.,* **55** (89), 101–118.
Militello, A., 1998: Hydrodynamics of shallow, wind-dominated embayments. Ph.D. dissertation, Florida Institute of Technology, 232 pp.
——, 2000: Hydrodynamic modeling of a sea-breeze dominated embayment, Baffin Bay, Texas. *Proc. Sixth Int. Conf. on Estuarine and Coastal Modeling,* New Orleans, LA, American Society of Civil Engineers, 795–810.
Parker, B. B., 1991: The relative importance of the various nonlinear mechanisms in a wide range of tidal interactions (review). *Tidal Hydrodynamics,* B. B. Parker, Ed., John Wiley and Sons, 237–268.
Prandle, D., 1991: Tides in estuaries and embayments (review). *Tidal Hydrodynamics,* B. B. Parker, Ed., John Wiley and Sons, 125–152.
Smith, N. P., 1979: Tidal dynamics and low-frequency exchanges in the Aransas Pass, Texas. *Estuaries,* **2** (4), 218–227.
——, 1985: Numerical simulation of bay–shelf exchanges with a one-dimensional model. *Contrib. Mar. Sci.* **28,** 1–13.
——, 1988: The Laguna Madre of Texas: Hydrography of a hypersaline lagoon. *Hydrodynamics of Estuaries.* B. Kjerfve, Ed., Vol. II, *Estuarine Case Studies,* CRC Press, 32–40.
Speer, P. E., and D. G. Aubrey, 1985: A study of nonlinear propagation in shallow inlet/estuarine systems. Part II: Theory. *Estuarine Coastal Shelf Sci.,* **21,** 207–224.
——, ——, and C. T. Friedrichs, 1991: Nonlinear hydrodynamics of shallow tidal inlet/bay systems. *Tidal Hydrodynamics,* B. B. Parker, Ed., John Wiley and Sons, 321–339.
Uncles, R. J., 1981: A note on tidal asymmetry in the Severn Estuary. *Estuarine Coastal Shelf Sci.,* **13,** 419–432.
Wu, J., 1980: Wind-stress coefficients over sea surface near neutral conditions—A revisit. *J. Phys. Oceanogr.,* **10,** 727–740.
Zetler, B. D., 1971: Radiational ocean tides along the coasts of the United States. *J. Phys. Oceanogr.,* **1,** 34–38.
——, and D. V. Hansen, 1970: Tides in the Gulf of Mexico—A review and proposed program. *Bull. Mar. Sci.,* **20** (1), 57–69.